Crystallization of Micelles at Chemically Terminated Interfaces

Max Wolff,* Uwe Scholz, Rainer Hock, and Andreas Magerl
Lehrstuhl für Kristallographie und Strukturphysik, Universität Erlangen-Nürnberg, D 91054 Erlangen, Germany

Vincent Leiner and Hartmut Zabel
Lehrstuhl für Experimentalphysik/Festkörperphysik, Ruhr-Universität Bochum, D 44780 Bochum, Germany
(Received 15 December 2003; published 21 June 2004)

In aqueous solutions and for high concentrations triblock copolymers are known to aggregate. As a critical volume fraction of micelles is reached they crystallize. We report on grazing incident small angle neutron scattering as an experimental tool to investigate the crystallization of spherical polymer micelles in the immediate vicinity of a flat solid interface. We find for an attractive surface potential a face centered close packed structure with a random orientation perpendicular to the normal of the interface. For a repulsive potential crystallization is suppressed.

DOI: 10.1103/PhysRevLett.92.255501 PACS numbers: 61.25.Hq, 61.12.Ha, 68.08.De

Thin polymer films are expected to play a key role in the fabrication of nanodevices as they can self-assemble at the molecular scale in the vicinity of solid substrates [1–5]. The structural ordering is correlated to the different interaction of different blocks of the polymer with the solid interface. For an attractive potential surface enrichment [6,7] and formation of lamellar phases parallel to the interface [8] have been found. The orientation of the lamellar can be changed by tuning the surface potential [9,10]. On the other hand, as the interaction between spherical polymer micelles can be varied continuously by changing the temperature, concentration, or pressure, they offer a model system for the study of gelation, percolation, crystallization, or the glass transition [11–15]. Recently some conclusions on the lateral pattern of adsorbed micelles have been drawn from off specular neutron reflectivity measurements [16], but the structure could not be resolved and the interpretation remained rather speculative. In the present study, we characterize for the first time the crystallization of spherical micelles from bulk solution close to flat solid interfaces with different surface potentials. We demonstrate that by combining the techniques of neutron reflectivity and small angle scattering in one experiment the structure of buried adsorbed layers can be resolved in three dimensions over length scales reaching from the nm to the μm regime.

The sample, Pluronic F127 (EO_{99}-PO_{65}-EO_{99}), was obtained from BASF Wyandotte Corp. (New Jersey, USA) and used without further purification. The bulk properties of similar samples are known in great detail [17]. Pluronics have a core of propyleneoxid (PO) with two terminations of ethyleneoxide (EO) and can self-assemble in aqueous solutions [11,18–21]. The resulting agreggations have a hydrophobic core and a hydrophilic shell. Theoretically these isotropic particles can be treated by the "core and gown" model [11–13]. For a critical micelle volume fraction a percolation transition is observed [12,14,15]. It is proposed that the percolated state is metastable, and the micelles crystallize when the system is disturbed, e.g., by the application of shear or at a solid interface [12]. The shear induced crystallization has been observed experimentally by small angle scattering [22,23]. Close to a hydrophilic interface the micelles are adsorbed in layers from the liquid phase when the percolation transition is approached [24,25]. For our experiment F127 was diluted to 20% (in weight) in deuterated water and filled into the sample cell in the liquid phase to prevent shearing of the percolated phase before the measurement.

Two single crystalline polished silicon disks were prepared as solid interfaces. One was oxidized for 15 min in a 5:1 mixture of H_2SO_4 and H_2O_2 resulting in a hydrophilic SiO_2 termination (contact angle of water 33°). The second substrate was cleaned with the same mixture of acids, and a deposition by exposure to gaseous HDMS (1,1,1,3,3,3-Hexamethyldisiazane) was made for 24 h to achieve a hydrophobic termination (contact angle of water 75°) [26].

With grazing incident small angle neutron scattering (GISANS) correlations parallel to an interface can be probed on an angstrom length scale [27,28]. Figure 1 illustrates the scattering geometry. A monochromatic neutron beam (marked by arrows, dashed inside the silicon) enters a silicon block from the side and becomes scattered at the solid-liquid interface. The intensity is registered by a position-sensitive detector. The **x**, **y**, and

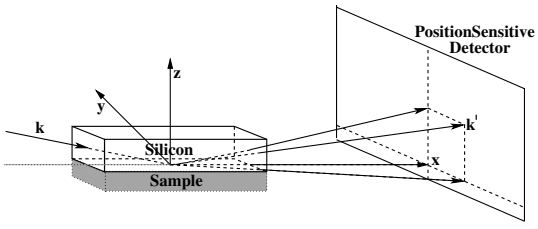

FIG. 1. Scattering geometry for GISANS studies. After scattering at the solid-liquid interface the neutrons are detected by a position-sensitive detector.

z directions are defined with respect to the surface of the sample, with **z** the normal of the interface, **x** in the plane of the interface and that defined by the incident beam direction **k**, and **y** perpendicular to **x** and **z**.

The measurements were carried out with the instrument ADAM at the Institut Laue-Langevin (Grenoble, France) using an incoming wavelength of $\lambda = 4.41$ Å $\pm$ 1%. For a momentum transfer of $|Q| = 0.04$ Å the resolution $\Delta Q_x = 1 \times 10^{-5}$ Å^{-1} is determined by the pixel size of the detector and the scattering angle. The resolution $\Delta Q_y = 3.8 \times 10^{-3}$ Å^{-1} and $\Delta Q_z = 7.5 \times 10^{-4}$ Å^{-1} is given by horizontal and vertical slits.

Figure 2 shows the specular reflected intensity taken with the sample in the liquid phase at 295 K at the hydrophilic (left panel) and the hydrophobic (right panel) interface. Both data sets are compared to the Fresnel reflectivity. The data are corrected for the small angle scattering (SAS) by substracting the intensity for an offset angle of $\omega = 0.3°$, defined as the difference between the incident and exit angles with respect to the sample surface. At $Q_z = 0.04$ Å, the intensity is increased for the hydrophilic interface, showing layers of adsorbed micelles. For the hydrophobic interface the reflectivity drops faster than R_F and no peak is visible. This shows a huge interface roughness and no adsorption of micelles. The inset in the left panel shows the rocking curve, including the SAS, taken at $Q_z = 0.04$ Å^{-1}, for the hydrophilic interface. The narrow peak at $\omega = 0$ is resolution limited and represents in-plane correlations over a length scale exceeding 60 μm. The broad component arises from the liquid structure factor of the bulk sample. The asymmetry of the intensity particularly well visible for offset angles $|\omega| > 0.5°$ originates from the reduced penetration depth D_p (depth for which the intensity has dropped to $1/e$) for negative ω values. The dashed line shows D_p calculated for $\beta = \frac{\lambda\rho\sigma}{4\pi} = 10^{-8}$ according to Ref. [29], with ρ the density and σ the sum of the absorption and the incoherent scattering cross sections.

Figure 3 shows GISANS data taken at an incident angle of 0.30°, slightly larger than the total reflection edge (0.25°), resulting in a penetration depth of the neutrons in the liquid of 40 μm. The total sample thickness was 1 mm. The panels on the top [3(a)–3(c)] and bottom [3(d)–3(f)] show data for the hydrophilic and the hydrophobic interfaces, respectively. All data are corrected for the critical angle $Q_z = \sqrt{Q_{z,m}^2 - 4\pi(\sigma_L - \sigma_{Si})}$, where $Q_{z,m}$ denotes the measured momentum transfer in the **z** direction and σ_L and σ_{Si} are the coherent scattering length densities of the liquid and the silicon, respectively.

For the left panels the sample is in the liquid phase at a temperature of 295 K. A ring of increased intensity with radius 4×10^{-2} Å^{-1} is visible for both interfaces, corresponding to the mean distance between micelles of 160 Å. At the hydrophilic interface sharp Bragg reflections become visible when the sample is heated to 298 K. The dots in the left panel of Fig. 4 show the reciprocal lattice for a cubic close packed (ccp) structure with the [111] direction perpendicular to the interface. When the perpendicular axes [1 − 10] and [11 − 2] are randomly oriented around the unique direction [111], the dots become smeared out along the solid and dashed circles. This structure corresponds to a two-dimensional powder known, e.g., from highly oriented pyrolytic graphite. Note that in our scattering geometry $|\mathbf{k}| \approx 100 \times |Q^{111}|$, and thus the Ewald sphere cuts through these powder rings (Fig. 4). The diffraction peaks visible in Fig. 3 are shown as solid circles in Fig. 4, while reciprocal lattice points not probed by the experiment are shown as dashed lines. The absolute Q values and angles to the [111] direction found in the experimental data are given in Table I and agree well with the calculated values. The intensities of the observed diffraction peaks decrease by three factors: first, an increasing diameter of the powder circles; second, the drop-off of the form factor (Fig. 5, left panel), which has been calculated from the "core and gown" model [11,21] for a core radius of 65 Å, a Gaussian width of 86 Å, and a polymer volume fraction of 95% in the micelle core; third, an increasing distance of the reciprocal lattice points from the Ewald sphere (Fig. 4, right side). Only

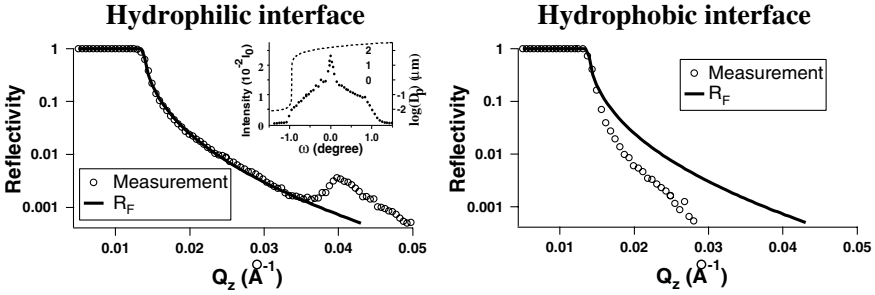

FIG. 2. Reflectivity data taken with the sample in the liquid phase in contact with a hydrophilic (left panel) and a hydrophobic (right panel) interface compared to the Fresnel reflectivity R_F. For the hydrophilic interface a reflection from adsorbed micelle layers is visible at $Q_z = 0.04$ Å^{-1}. The inset in the left panel shows a rocking scan of this reflection. The dashed line is the calculated neutron penetration depth.

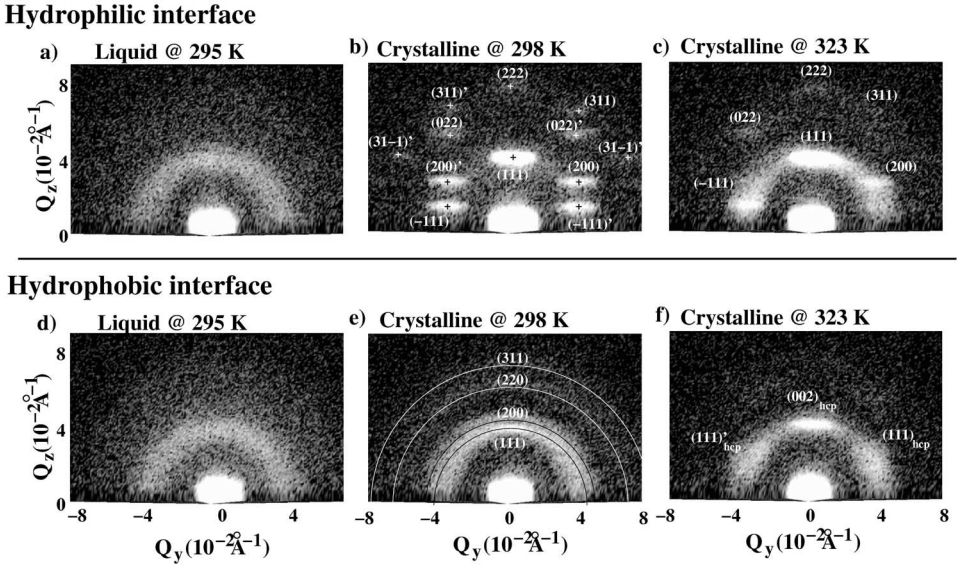

FIG. 3. GISANS data taken at a hydrophilic (a)–(c) and a hydrophobic (d)–(f) interface in the liquid phase at 295 K (a),(d) and in the crystalline phase at 298 K (b),(e) and 323 K (c),(f).

the smearing of the reflections due to mosaicity or due to the size of the crystallites contributes to the detected intensity.

The data for the hydrophobic interface at 298 K feature four diffraction rings. Their absolute positions are explained by a three-dimensional polycrystalline cubic face centered structure with a lattice constant of 295 Å (Table I). A similar structure was found earlier in the bulk [30]. When the temperature is increased to 323 K [3(c)], we find the sample at the hydrophilic interface to become textured, and a rotational orientation develops with respect to the common axis. At these temperatures different reflections emerge also for the hydrophobic interface. These are explained by a hexagonal close packing (hcp) (Fig. 4) again with random in-plane orientation. The smearing of the $(111)_{\mathrm{hcp}}$ shows the presence of staple faults as the hcp develops from a cubic lattice.

For the (111) $[(002)_{\mathrm{hcp}}]$ reflection at $Q_z = 0.037$ Å a rocking scan (right panel in Fig. 5) shows that for the hydrophilic interface the line shape consists of two components as found, e.g., for epitaxial niobium on sapphire substrates [31]. These indicate two different length scales that need to be considered. The narrow component reveals long range orientational correlations of at least 60 μm or 2000 unit cells. The wider component results from the mosaicity and the size of the crystallites. For increasing temperature the broad component decreases while the amplitude of the narrow one becomes predominant. We assign this intensity swapping to the annealing of the sample directly related to the formation of texture with respect to the rotation of crystallites around the common axis. For the hydrophobic interface the diffuse intensity is much weaker and the narrow component is missing. This shows that crystallization is suppressed at the hydrophobic interface and no long range orientational correlations can be built up. Thus, an amorphous rather than a crystalline structure is formed. For the (111) $[(002)_{\mathrm{hcp}}]$ reflection the GISANS data were taken at an offset angle

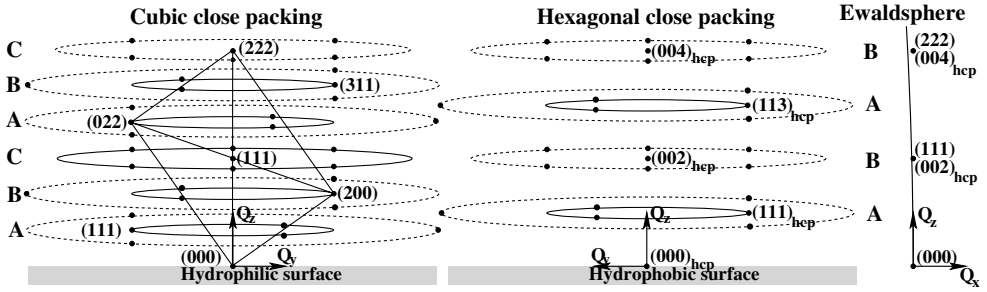

FIG. 4. Reciprocal lattice for a cubic (ccp) and a hexagonal (hcp) close packing. The dots mark the positions of reciprocal lattice points. For a two-dimensional powder with the unique axis along Q_z perpendicular to the interface these points are smeared out into circles. On the right side the positions of the Bragg reflections in the **z** direction are shown with respect to the Ewald sphere.

TABLE I. Position of the Bragg reflections.

(*hkl*)	$\lvert Q\rvert/0.037$ Å^{-1}	fcc	Angle to (111)	fcc
(111)	1 ± 0.05	1	0	0°
(-111)	1 ± 0.05	1	70 ± 2	70.5°
(200)	1.15 ± 0.02	$\sqrt{\frac{4}{3}} \approx 1.15$	53 ± 2	54.7°
(220)	1.59 ± 0.07	$\sqrt{\frac{8}{3}} \approx 1.63$	33 ± 2	35.3°
(311)	1.82 ± 0.12	$\sqrt{\frac{11}{3}} \approx 1.91$	27 ± 2	29.5°
$(31-1)$	1.82 ± 0.12	$\sqrt{\frac{11}{3}} \approx 1.91$	57 ± 2	58.5°
(222)	1.89 ± 0.12	2	0	0

of $\omega = -0.85°$ (marked by the arrow in Fig. 5). Thus, only the outer tail of the reflection for the hydrophilic interface contributes to the intensity detected in the GISANS measurement. Note that for our system we can exclude the formation of surface micelles as they would show up in the specular reflectivity shown in Fig. 2. The adsorption results from the interaction of the micelles with the surface potential of the hard wall.

In summary, we have characterized the effect of different surface potentials on the crystallization of spherical micelles at flat solid interfaces. With GISANS, length scales from the nanometer up to micrometer range have been addressed: we find that micelles with a hydrophilic shell crystallize in a cubic face centered lattice (lattice constant 29.5 nm) at a hydrophilic interface and with in-plane correlations exceeding 60 μm. When crossing the percolation limit, first a 2D powder with a ccp structure is formed distinguished by an unique axis perpendicular to the interface. For higher temperatures a rotational alignment of crystallites around the common axis develops. For the hydrophobic interface crystallization neglects the interface and a three-dimensional powder forms with correlations only on short length scales. It transforms into a hcp structure with increasing temperature. In conclusion, we have shown that the structural arrangement of spherical micelles at flat surfaces is strongly affected by the surface potential. Furthermore, GISANS was found to be an excellent tool to gain information on the near surface structure of particles that are adsorbed from the solution at the solid interface. This opens a new possibility to test theoretical predictions for supercooled liquids and may also have an impact on technical applications.

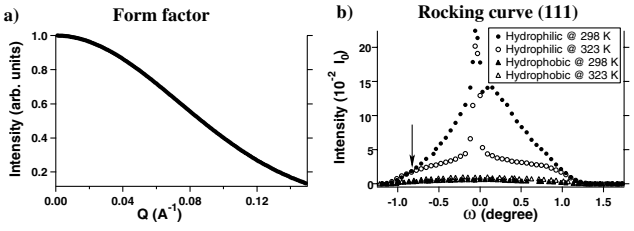

FIG. 5. Form factor (left panel) for the F127 micelles and rocking scan of the (111) Bragg reflection at $Q_z = 0.037$ Å^{-1} (right panel) for the hydrophilic (circles) and the hydrophobic (triangles) interface in the crystalline phase at temperatures of 298 K (solid symbols) and 313 K (open symbols). The arrow marks the position at which the GISANS data were taken.

We acknowledge financial support of the DFG (MA161/4 and ZA801/17) and the BMBF (ADAM 04ZAE8BO) and appreciate fruitful discussions with H. Zimmermann.

*Present address: Institut Laue-Langevin, 38042 Grenoble, France.
Electronic address: v-wolff@ill.fr

[1] S. Ludwigs *et al.*, Nature Mater. **2**, 744 (2003).
[2] R. A. Register, Nature (London) **424**, 378 (2003).
[3] S. O. Kim *et al.*, Nature (London) **424**, 411 (2003).
[4] C. De Rosa *et al.*, Nature (London) **405**, 433 (2000).
[5] J. Y. Cheng *et al.*, Appl. Phys. Lett. **81**, 3657 (2002).
[6] R. A. L. Jones *et al.*, Phys. Rev. Lett. **62**, 280 (1989).
[7] G. H. Fredrickson, Macromolecules **20**, 2535 (1987).
[8] S. H. Anastasiadis *et al.*, Phys. Rev. Lett. **62**, 1852 (1989).
[9] G. J. Kellogg *et al.*, Phys. Rev. Lett. **76**, 2503 (1996).
[10] E. Huang *et al.*, Macromolecules **31**, 7641 (1998).
[11] L. Lobry *et al.*, Phys. Rev. E **60**, 7076 (1999).
[12] W.-R. Chen, S.-H. Chen, and F. Mallamace, Phys. Rev. E **66**, 021403 (2002).
[13] J. Bergenholtz and M. Fuchs, Phys. Rev. E **59**, 5706 (1999).
[14] J. Noolandi, A.-C. Shi, and P. Linse, Macromolecules **29**, 5907 (1996).
[15] F. Mallamace *et al.*, Phys. Rev. Lett. **84**, 5431 (2000).
[16] D. J. McGillivray *et al.*, Langmuir **19**, 7719 (2003).
[17] K. Mortensen, Polym. Adv. Technol. **12**, 2 (2001).
[18] J. S. Pedersen and M. C. Gerstenberger, Colloids Surf. A **213**, 175 (2003).
[19] K. Mortensen, W. Brown, and B. Norden, Phys. Rev. Lett. **68**, 2340 (1992).
[20] P. Linse, Macromolecules **26**, 4437 (1993).
[21] Y. Liu, S.-H. Chen, and J. S. Huang, Macromolecules **31**, 2236 (1998).
[22] K. Mortensen, J. Phys. Condens. Matter **8**, A103 (1996).
[23] E. Eiser *et al.*, Phys. Rev. E **61**, 6759 (2000).
[24] M. C. Gerstenberg, J. S. Pedersen, and G. S. Smith, Phys. Rev. E **58**, 8028 (1998).
[25] M. C. Gerstenberg, J. S. Pedersen, and J. Majewski, Langmuir **18**, 4933 (2002).
[26] W.W.Carr *et al.*, in National Textil Center Annual Report, 2001.
[27] W. A. Hamilton *et al.*, Phys. Rev. Lett. **72**, 2219 (1994).
[28] P. Müller-Buschbaum, R. Cubitt, and W. Petry, Langmuir **19**, 7778 (2003).
[29] L. G. Parratt, Phys. Rev. **95**, 359 (1954).
[30] C. Wu *et al.*, Macromolecules **30**, 4574 (1997).
[31] A. R. Wildes, J. Mayer, and K. Theis-Bröhl, Thin Solid Films **401**, 7 (2001).